Smith, M. D., Field, D. E., Yuan, C., Pomeroy, J. W., Uren, M. J., Kuball, M. H. H., & al., E. (2020). GaN-on-diamond technology platform: Bonding-free membrane manufacturing process. *AIP Advances*, *10*(3), [035306]. https://doi.org/10.1063/1.5129229

Publisher's PDF, also known as Version of record

License (if available):
CC BY

Link to published version (if available):
10.1063/1.5129229

Link to publication record in Explore Bristol Research
PDF-document

This is the final published version of the article (version of record). It first appeared online via AIP Publishing at https://aip.scitation.org/doi/pdf/10.1063/1.5129229?download=true . Please refer to any applicable terms of use of the publisher.

University of Bristol - Explore Bristol Research

General rights

This document is made available in accordance with publisher policies. Please cite only the published version using the reference above. Full terms of use are available: http://www.bristol.ac.uk/pure/about/ebr-terms

Kuball, M. H. H., Field, D. E., Yuan, C., Uren, M. J., & Pomeroy, J. W. (2020). GaN-on-diamond technology platform: Bonding-free membrane manufacturing process. *AIP Advances*.

Link to publication record in Explore Bristol Research
PDF-document

University of Bristol - Explore Bristol Research

General rights

This document is made available in accordance with publisher policies. Please cite only the published version using the reference above. Full terms of use are available: http://www.bristol.ac.uk/pure/about/ebr-terms

ACCEPTED MANUSCRIPT
AIP Advances
This is the author's peer reviewed, accepted manuscript. However, the online version of record will be different from this version once it has been copyedited and typeset.
PLEASE CITE THIS ARTICLE AS DOI:10.1063/1.5129229
AIP Publishing

GaN-on-diamond technology platform: Bonding-free membrane manufacturing process

Matthew D. Smith[1], Jerome A. Cuenca[2], Daniel E. Field[3], Yen-chun Fu[1], Chao Yuan[3], Fabien Massabuau[4], Soumen Mandal[2], James W. Pomeroy[3], Rachel A. Oliver[4], Michael J Uren[3], Khaled Elgaid[2], Oliver A. Williams[2], Iain Thayne[1], Martin Kuball[3,a]

[1]*School of Engineering, University of Glasgow, Glasgow, G12 8LT, United Kingdom*

[2]*School of Engineering, Cardiff University, Cardiff, CF24 3AA, United Kingdom*

[3]*Center for Device Thermography and Reliability (CDTR), H.H. Wills Physics Laboratory, University of Bristol, Bristol, BS8 1TL, United Kingdom*

[4]*Department of Materials Science and Metallurgy, University of Cambridge, 27 Charles Babbage Road, Cambridge, CB3 0FS, United Kingdom*

GaN-on-diamond samples were demonstrated using a membrane-based technology. This was achieved by selective area Si substrate removal of areas up to 1 cm × 1 cm from a GaN-on-Si wafer, followed by direct growth of polycrystalline diamond using microwave plasma chemical vapour deposition on etch exposed N-polar AlN epitaxial nucleation layers. Atomic force microscopy and transmission electron microscopy were used to confirm the formation of high quality, void-free AlN/diamond interfaces. The bond between the III-nitride layers and diamond was validated by strain measurements of the GaN buffer layer. Demonstration of this technology platform is an important step forward for the creating of next generation high power electronic devices.

Transistors created on the GaN-on-diamond material system have attracted significant interest in recent years due to their increased high frequency and high power handling potential, when compared to commercially established GaN-on-SiC technologies. The high thermal conductivity of polycrystalline diamond substrates significantly improves thermal transistor management, increasing by up to ~3x the power density handling capability of GaN-based radio-frequency (RF) devices [1]. This performance benefit can be utilized to increase RF transmitter output power as required for next generation (5G and beyond) wireless communication systems with enhanced reliability. The current GaN-on-diamond state-of-the-art fabrication

---

[a)] Author to whom correspondence should be addressed. Electronic mail: Martin.Kuball@bristol.ac.uk.

ACCEPTED MANUSCRIPT
AIP Advances
This is the author's peer reviewed, accepted manuscript. However, the online version of record will be different from this version once it has been copyedited and typeset.
PLEASE CITE THIS ARTICLE AS DOI:10.1063/1.5129229
AIP Publishing

process uses amorphous dielectric interlayers as seed layers for diamond growth [1-6], following wafer bonding to a temporary carrier wafer [4, 7-9] and additional processing. The inclusion of a wafer bonding stage both increases manufacturing complexity and potentially compromises the device surface, negatively impacting device performance.

In this work, we describe a membrane-based GaN-on-diamond production methodology which obviates the need for bonding to a carrier wafer. Polycrystalline diamond is deposited directly on membranes formed from GaN-on-Si wafers by selective area substrate removal, enabling the growth of 50 µm thick crack-free diamond directly on the exposed back-side (N-polar face) of AlN epitaxial nucleation layers. The simplified production method provides a route to GaN-on-diamond devices and circuits with improved performance and manufacturability.

AlGaN/GaN heterostructures were grown by metalorganic chemical vapour deposition on 1 mm thick Si substrates of diameter 150 mm. High quality GaN growth is initiated via an AlN nucleation layer (200 nm), followed by AlGaN strain relief layers (~5 µm) used to manage stress occurring due to differences in the coefficients of thermal expansion between Si and III-nitride layers during the growth cooldown [10]. A 1.5 µm thick GaN buffer layer, the lower 1 µm of which was C-doped, was grown above the AlGaN strain relief layers. This was capped with an $Al_{0.2}Ga_{0.8}N$ barrier (20 nm) and a GaN surface layer (3 nm). Wafers were scribed using a mechanical saw to produce 12 mm x 12 mm square samples and then subjected to a high power (900 W) inductively-coupled plasma (ICP) SF_6/C_4F_8 modified Bosch etch process [11], thinning the Si substrate to 150 µm. A reduced power (600 W) ICP SF_6/C_4F_8 Bosch etch was used to remove the remaining Si substrate in selected areas (defined using photolithography), with in-situ end-point interferometry employed to determine the etch duration. This process, depicted in Fig. 1, results in III-nitride membranes surrounded by Si supports. The etch exposed N-polar AlN membrane surfaces were imaged using atomic force microscopy (AFM).

Figure 1. Process schematic showing (a) GaN-on-Si sample (b) substrate thinning by plasma etching (c) formation of III-nitride membranes by plasma etching and (d) GaN-on-diamond membranes.

Diamond growth was achieved using a Carat systems CTS6U microwave plasma chemical vapour deposition (MPCVD) reactor. Prior to growth, a modified diamond-on-AlN seeding process was used, similar to that found in [12]. The exposed III-nitride membranes were first pre-treated in a N_2/H_2 microwave plasma with a forward power of 1.5 kW at 20 Torr. A nano-diamond colloid solution was then pipetted onto the substrates, which were rinsed carefully in de-ionized water and dried on a hotplate for 10 minutes at 115°C. After seeding, diamond growth was achieved in a CH_4/H_2 microwave plasma with a power of 5.0-5.5 kW at 110-120 Torr and a CH_4 concentration of 3% in a 500 sccm flow rate. With a typical growth rate at

AIP Advances ACCEPTED MANUSCRIPT
This is the author's peer reviewed, accepted manuscript. However, the online version of record will be different from this version once it has been copyedited and typeset.
PLEASE CITE THIS ARTICLE AS DOI:10.1063/1.5129229
AIP Publishing

these conditions of approximately 2-3 μm/hour, growth runs were conducted for at least 24 hours to ensure a diamond thickness of over 50 μm. The temperature of the sample during growth was monitored using a Williamson dual wavelength pyrometer. The samples were then cleaned in organic solvents to remove carbon contamination deposited during diamond growth.

The interface between the diamond and AlN was imaged using scanning transmission electron microscopy (STEM). The sample was lifted out of the membrane region from the III-nitride face using an FEI Helios Nanolab focused ion beam (FIB), and high-angle annular dark field STEM (HAADF-STEM) images were taken on a FEI Osiris microscope operated at 200 kV. Raman spectroscopy was carried out on both the III-nitride surface and the diamond using a Renishaw InVia system with a 488 nm laser excitation source.

Figure 2. (a) Multiple GaN-on-Si membranes on a single sample (b) large area membrane with aspect ratio ~10^3 (c) optical microscope image (5x) of III-nitride membranes with exposed N-polar AlN surfaces (d) AFM of N-polar AlN surface

Fig. 2 shows III-nitride membrane samples prior to diamond growth. A range of circular and squared membranes of varying sizes were produced, from 1 cm × 1 cm squares (Fig. 2(b)) to 0.5 mm diameter circles (Fig. 2(c)), the former representing an aspect ratio of ~ 10^3 considering a total III-nitride layer thickness of ~ 7 µm. The ICP power reduction during the etching steps of the Bosch processes described above was found to be essential to prevent cracking of the membranes. Complete removal of the Si substrate was verified by a characteristic increase in surface reflectivity as monitored by in-situ interferometry, and the high optical reflectivity of the exposed III-nitride surfaces relative to the remaining Si support structure enabled rapid visual inspection. The exposed N-polar AlN nucleation layer surfaces had an rms roughness of 0.9 nm over a 2 µm × 2 µm area, as measured by AFM, illustrated in Fig. 2(d). The surface morphology and roughness are comparable to recent works exploring N-polar AlN for optoelectronics applications [13].

Figure 3: Membrane samples (a) during and (b) after diamond growth (c) optical microscope image (5x) of membranes after diamond growth

Figs. 3(a) and (b) show the membrane sample from Fig. 2(a) during and after diamond growth, respectively, with no macro-scale deformation noticeable. Diamond growth temperature as measured using in-situ pyrometry varied between 700 to 800 °C, although this method only provides a spot measurement on the sample and some inhomogeneity in the diamond is apparent from Fig 3(b). This is attributed to the elliptical plasma density profile and electric field focusing around the sample corners, causing an increase in temperature and difference in growth conditions. Raman spectroscopy was used to quantify the

ACCEPTED MANUSCRIPT
AIP Advances
This is the author's peer reviewed, accepted manuscript. However, the online version of record will be different from this version once it has been copyedited and typeset.
PLEASE CITE THIS ARTICLE AS DOI:10.1063/1.5129229
AIP Publishing

quality and stress in the diamond across the sample. The diamond sp^3 peak was observed at an average position of 1332 ± 0.3 cm^{-1} with an average full width half maximum (FWHM) of 6.0 ± 1.0 cm^{-1}. These numbers correspond to diamond with a good crystal quality and negligible stress [14]. We note that Raman measurements made at points which were glowing red in Fig. 3(a), i.e. near the edges of the sample, had an increased FWHM (7.2 ± 1.0 cm^{-1}) compared to the other regions (5.3 ± 1.0 cm^{-1}), indicative of diamond regions with lower crystal quality and higher defect density, i.e., in the following we concentrate on the central regions of the sample. For the 0.5 mm diameter circular membranes, located in the central region of the sample, Fig. 3(c) shows that a continuous diamond layer has been deposited across both the III-nitride membrane and the Si border. In contrast, for the sample with a larger 1 cm × 1 cm square membrane, the thermal stresses induced when cooling from the growth temperature to room temperature resulted in the III-nitride membrane fracturing along the hexagonal crystal planes. This is attributed to a mismatch in coefficient of thermal expansion and elastic modulii of the III-nitride stack, the silicon frame and the diamond. Since the thermal expansion coefficient of diamond is much lower than that of the layers in the III-nitride stack, upon cooling the III-nitride layers are held in tension, and the membrane shatters if local stress values exceed the tensile yield strength. The actual practical limitations on membrane dimensions require further investigation, and it is suspected that rounded edges may mitigate local stress exceeding mechanical yield values [15].

Figure 4: (a) Raman spectra taken at the center (0.4 GPa, blue line) and the bottom (1 GPa, red line) of the membrane. (b) the variation in stress across a membrane. Maximum error of 10% for these values estimated from the fitting error using the bootstraps method.

For 0.5 mm diameter circular membranes (Fig. 3(c)), Raman spectroscopy measurements (Fig. 4(a)) confirmed the presence of tensile, biaxial stress in the GaN buffer layers in every membrane measured, reaching a maximum of 1 GPa at the edges of the membranes (Fig. 4(b)). The standard relationship between the stress induced Raman peak shift and biaxial stress is used [16], with reference to the relaxed GaN E_2 phonon frequency value of 567.2 cm^{-1} [17]. The final stress in the GaN film depends on in-built stress at the diamond deposition temperature and geometric effects such as bowing, buckling and clamping at the rim of the membrane which has a non-trivial solution. To determine an approximated thermomechanical stress we can assume a flat membrane and uniform biaxial stress and apply the equation $\Delta\sigma = E \cdot \Delta\alpha \cdot \Delta T/(1-\nu)$, where $\Delta\sigma$ is the change in stress, $E = 295$ GPa [18] and $\nu = 0.35$ are the Young's modulus and Poisson ratio of GaN, respectively, and $\Delta\alpha = 1.85\times10^{-6}$ K^{-1} is the average difference in thermal expansion coefficient between the GaN film [19] and diamond [20] over the temperature range $\Delta T = 800$°C, e.g., subtracting the ambient temperature from the diamond deposition temperature. A biaxial tensile stress value of ~ 0.7 GPa was determined using this expression. This approximate value lies within the range measured across a membrane by Raman spectroscopy (Fig 4(b)). The presence of tensile stress is indicative of a strong bond between the diamond

AIP Advances ACCEPTED MANUSCRIPT
This is the author's peer reviewed, accepted manuscript. However, the online version of record will be different from this version once it has been copyedited and typeset.
PLEASE CITE THIS ARTICLE AS DOI:10.1063/1.5129229
AIP Publishing

and the III-nitride structure, which can withstand such large stresses. If the III-nitride membrane was delaminated from the diamond, the GaN layer would be more relaxed which is not observed.

Figure 5. Cross-sectional STEM showing (a) the III-nitride epistructure (AlN nucleation, AlGaN strain relief and GaN buffer layers) and diamond, with a higher contrast inset highlighting diamond columnar growth (b) close up of the diamond/AlN interface

A high-quality diamond/AlN interface is observed in 0.5 mm diameter circular membranes using STEM (Fig. 5(a) and (b)), with no voids or cracks visible, confirming the presence of a strong bond. The scale of the interfacial roughness broadly correlates with N-polar AlN surface morphology after Si substrate removal shown in Fig. 2(d), which seems to have been preserved following diamond growth. At the early stages, heteroepitaxial diamond growth follows the Volmer-Weber mechanism, three-dimensional growth of diamond islands, until sufficient lateral growth results in film coalescence followed by columnar growth highlighted in Fig. 5(a).

We note that in the present structure there is a low thermal conductivity AlGaN strain relief layer between the GaN where transistor current would flow and the diamond. Removing this AlGaN layer is ultimately important for efficient heat transport between a device channel heat source and the diamond substrate. In this work, we have shown that seeding the AlN layer initiates diamond growth which is strongly bonded. There is no technological barrier to the incorporation of an AlN "initiation" layer into the GaN buffer close to the device channel [21], which can be accessed via the plasma etching methods described previously in combination with highly selective removal of GaN, stopping on the AlN [22]. This is the next step to the realization of high power density GaN RF devices [1], with improved output power and reliability.

In conclusion, cross-sectional STEM and Raman spectroscopy analyses confirm the establishment of a method to strongly bond high quality MPCVD deposited polycrystalline diamond to N-polar III-nitride membranes formed from GaN-on-Si wafers by selective area substrate removal. The approach obviates the need for wafer bonding and thus provides a route to GaN-on-diamond devices and circuits with improved manufacturability.

ACKNOWLEDGMENTS

The authors would like to acknowledge financial support of the Engineering and Physical Sciences Research Council (EPSRC) under the program Grant GaN-DaME (EP/P00945X/1).

AIP Advances ACCEPTED MANUSCRIPT
This is the author's peer reviewed, accepted manuscript. However, the online version of record will be different from this version once it has been copyedited and typeset.
PLEASE CITE THIS ARTICLE AS DOI:10.1063/1.5129229
AIP Publishing

DATA AVAILABILITY

The data that support the findings of this study are available from the corresponding author, Prof. M. Kuball, at the University of Bristol, upon reasonable request.

REFERENCES

[1] J. W. Pomeroy, R. B. Simon, H. Sun, D. Francis, F. Faili, D. J. Twitchen, and M. Kuball IEEE Elect Device L. **35** 1007 (2014)

[2] H. Sun, R. B. Simon, J. W. Pomeroy, D. Francis, F. Faili, D. J. Twitchen, and M. Kuball, Appl. Phys. Lett. **106**, 111906 (2015)

[3] T. Liu, Y. Kong, L. Wu, H. Guo, J. Zhou, C. Kong, and T. Chen, IEEE Electr Device L, **38** 1417 (2017)

[4] D. Francis, F. Faili, D. Babić, F. Ejeckam, A Nurmikko, and H. Maris, Diam Relat Mater. **19** 229 (2010)

[5] L. Yates, J. Anderson, X. Gu, C. Lee, T. Bai, M. Mecklenberg, T. Aoki, M. S. Goody, M. Kuball, E. L. Piner, and S. Graham, ACS Appl. Mater. Interfaces **10,** 24302 (2018)

[6] Y. Zhou, J. Anaya, J. W. Pomeroy, H. Sun, X. Gu, A. Xie, E. Beam, M. Becker, T. A. Grotjohn, C. Lee, and M. Kuball, ACS Appl. Mater. Interfaces, **9**, 34416 (2017)

[7] T. Gerrer, A. Graff, M. Simon-Najasek, H. Czap, T. Maier, F. Benkhelifa, S. Muller, C. Nebel, P. Waltereit, R. Quay and V. Cimalla, Appl. Phys. Lett. **114**, 252103 (2019)

[8] T. Gerrer, V. Cimalla, P. Waltereit, S. Muller, F. Benkhelifa, T. Maier, A. Graff, H. Czap, C. Nebel, and R. Quay in *12th European Microwave Integrated Circuits Conference (EuMIC)*, Nuremburg, Germany, 2017, pp. 25-28

[9] M. J. Tadjer, T. J. Anderson, M. G. Ancona, P. E. Raad, P. Komarov, T. Bai, J. C. Gallagher, A. D. Koehler, M. S. Goorsky, D. A. Francis, K. D. Hobart and F. J. Kub, IEEE Electr Device L, **40**, 881 (2019)

[10] C. Q. Chen, J. P. Zhang, M. E. Gaevski, H. M. Wang, W. H. Sun, R. S. Q. Fareed, J. W. Yang, and M. A. Khan, Appl. Phys. Lett. **81**, 4961 (2002)

[11] F. Laerme, A. Schilp, K. Funk and M. Offenberg, in *Technical Digest. IEEE International MEMS 99 Conference. Twelfth IEEE International Conference on Micro Electro Mechanical Systems*, Orlando, FL, USA, 1999, pp. 211-216

[12] S. Mandal, C. Yuan, F. Massabuau, J. W. Pomeroy, J. Cuenca, H. Bland, E. Thomas, D. Wallis, T. Batten, D. Morgan, R. Oliver, M. Kuball, and O. A. Williams, ACS Appl. Mater. Interfaces, **11**, 40826 (2019)

[13] Y. Hayashi, R. Katayama, T. Akiyama, T. Ito, and H. Miyake, Appl. Phys. Express **11,** 031003 (2018)

[14] S. Prawer and R. J. Nemanich, Philos. Trans. R. Soc. A Math. Phys. Eng. Sci., **362** 2537 (2004)

[15] R. J. Atkinson, W. J. Winkworth, and G. M. Norris, *Behaviour of Skin Fatigue Cracks at the Corners of Windows in a Comet I Fuselage*, (H.M. Stationary Office, London, 1962), p. 4

[16] F. Demangeot, J. Frandon, P. Baules, F. Natali, F. Semond, and J. Massies, Phys. Rev. B, **69**, 155215 (2004)

[17] C. -L. Hsiao, L. -W. Tu, T. -W. Chi, M. Chen, T. -F. Young, C. -T. Chia, and Y. -M. Chang, Appl. Phys. Lett., **90**, 043102 (2007)

[18] R. Nowak, M. Pessa, M. Suganuma, M. Leszczynski, I. Grzegory, S. Porowski and F. Yoshida, Appl. Phys. Lett. **75**, 2070 (1999)

[19] A. U. Sheleg and V. A. Savastenko, Vesti Akad. Nauk BSSR, Ser. Fiz. Mat. Nauk **3**, 126 (1976)

[20] M. J. Edwards, C. R. Bowen, D. W. E. Allsopp and A C E Dent, J. Phys. D: Appl. Phys. 43 385502 (2010)

[21] M. Kuball, J.W Pomeroy, M. Uren, O.A.A. Williams, A semiconductor on diamond substrate, precursor for use in preparing a semiconductor on diamond substrate, and methods for making the same. GB patent: GB 1814192.9, 2019

[22] S. A. Smith, C. A. Wolden, M. D. Bremser, A. D. Hanser, and R. F. Davis, Appl. Phys. Lett. **71**, 3631 (1997)

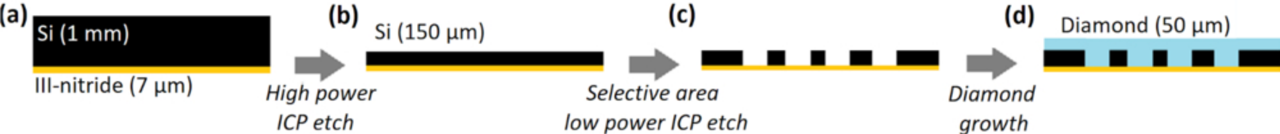

(a)
Si (1 mm)
III-nitride (7 μm)
High power
ICP etch
(b)
Si (150 μm)
Selective area
low power ICP etch
(c)
Diamond
growth
(d)
Diamond (50 μm)

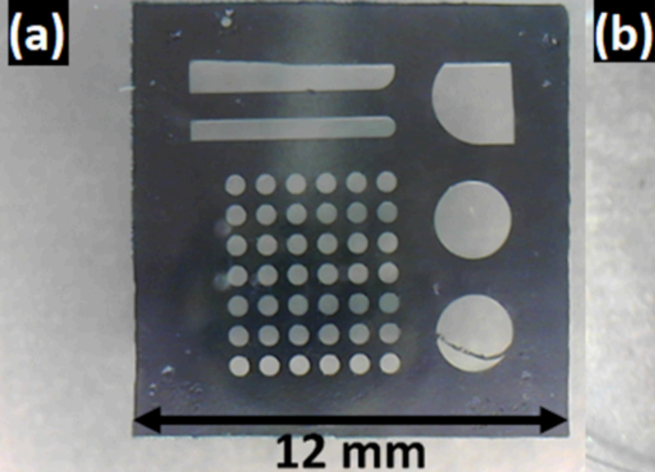
(a)
12 mm

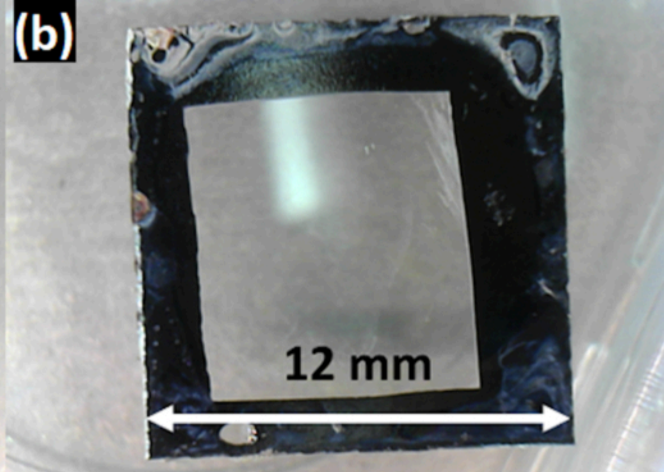
(b)
12 mm

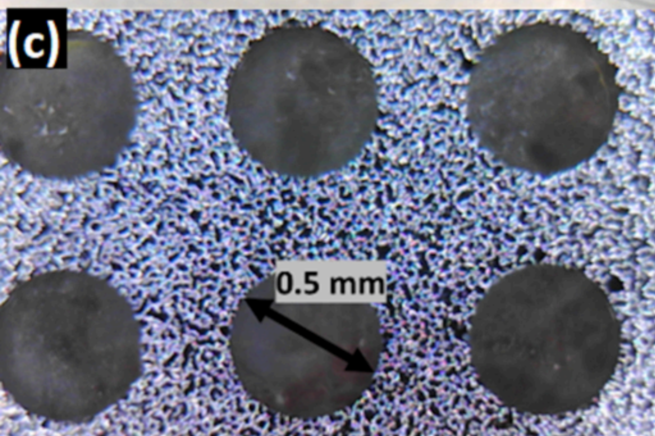
(c)
0.5 mm

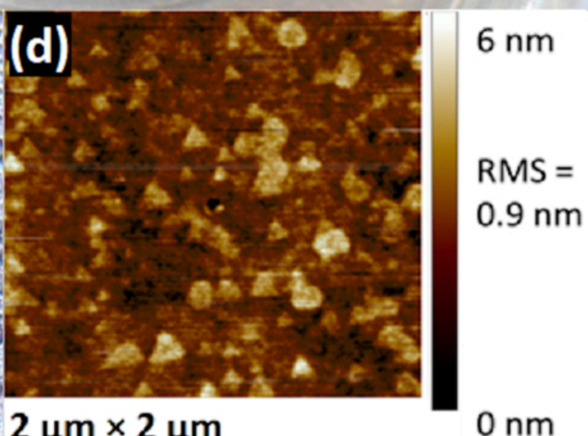
(d)
6 nm
RMS =
0.9 nm
0 nm
2 µm × 2 µm

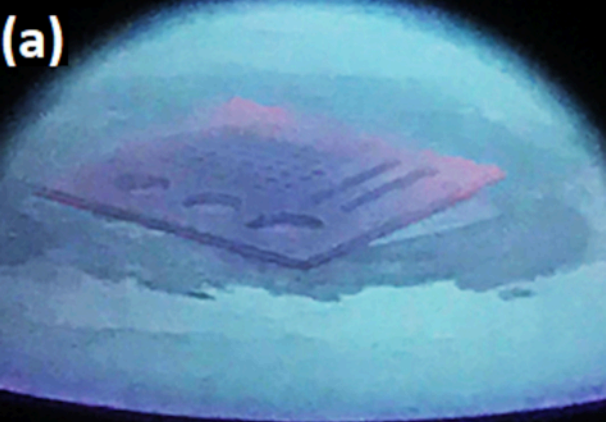
(a)

(b)
12 mm

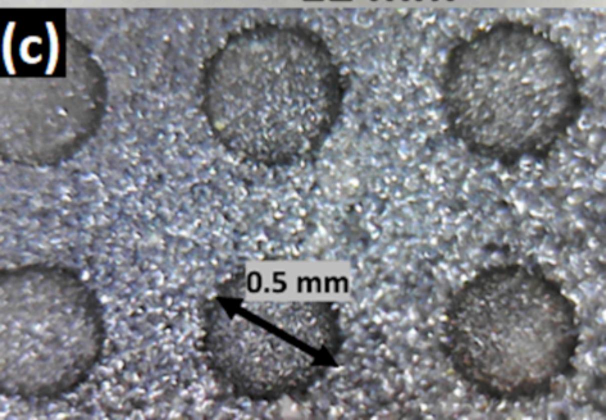
(c)
0.5 mm

(a)
Minimum Stress
Maximum Stress
Normalised Intensity
1
0.8
0.6
0.4
0.2
0
540
560
580
600
Raman Shift (cm^{-1})
(b)
1.0
0.9
0.8
0.7
0.6
0.5
0.4
Residual Stress (GPa)
100 μm

(a)

Diamond

Higher contrast

AlN

$Al_xGa_{1-x}N/Al_yGa_{1-y}N$

GaN

1 μm

(b)

Diamond

AlN

50 nm